

Determination of Calibration Cycles Using X-ray Tube Output, Workload and Use Factor for Diagnostic X-rays

Jermain Exeter and Petal Surujpaul*

Medical Physicist at Georgetown Public Hospital Corporation, University of Guyana, Guyana

*Corresponding author: Surujpaul PP, Department of Radiology, Medical Physicist at Georgetown Public Hospital Corporation, University of Guyana, East & Thomas Streets, North Cummingsburg, Georgetown, Demerara, Guyana, Tel: +1592-650-076; E-mail: psurujpaul@gmail.com

Received date: Feb 19, 2018; Accepted date: Mar 30, 2018; Published date: Apr 06, 2018

Copyright: © 2018 Exeter J, et al. This is an open-access article distributed under the terms of the Creative Commons Attribution License, which permits unrestricted use, distribution, and reproduction in any medium, provided the original author and source are credited.

Abstract

The stipulated standard time according to annual inspection done under the Health Facility Act 2008 is once per year however, due to varying workloads, use factor, and tube age the calibration cycles can be adjusted. Significance of this work includes determining the optimal calibration time of diagnostic X-ray tubes, resulting in promotion of new knowledge and influencing policies on the need for timely calibrations, additionally it may be used as a marker for urgent calibration in high workload facilities via diagnostic reference per unit to establish an institutional local standard. Parameters involved in this research are X-ray tube output (mGy/mAs), workload (mA-min/week), use factor and fluence (mGy/cm²). Comparative studies were done at two local hospitals in Guyana namely Georgetown Public Hospital Corporation (GPHC) and Linden Hospital Corporation (LHC). Barium meals (B.M) and intravenous pyelograms (IVP) were measured at Georgetown Public Hospital Corporation. The RaySafe X2 was placed in the path of the X-ray beam at different settings of peak kilovoltage and milliamperage- second and the radiation quantities were displayed on the base unit. This research investigated the effect of variation factor on the calibration of the static radiography on a fluoroscopy unit. Factors measured included kerma, tube output, fluence and age of tube output and workload. The differences obtained were significant in the cases of the elevated R/F sensor at 60 cm and at table top of 115 cm and varying peak kilovoltages and milliamperage. The difference in tube output could be attributed to anode surface damage (pitting), age of the tube, filtration, and collimation. A lower workload requires less calibration. In conclusion facilities with a workload of approximately 50 patients do not require more frequent calibration.

Keywords: Calibration; Workload; Fluence

Introduction

X-rays are extensively used in medicine for both diagnosis and therapy. Radiation doses due to conventional radiography depend on several operational conditions that include the X-ray unit, (anode and filter combinations), technical parameters (kV and mAs) beam qualities (HVL, homogeneity factor), geometry factors (focus to chamber distance), and the type of image receptor (Peixoto JCP). The incident air kerma and entrance surface air kerma are two important quantities in diagnostic X-ray radiology [1].

Parameters measured in this investigation included incident air kerma from the incident X-ray beam, at beam axis, at a certain source to image distance (SID). The unit of kerma is the same as the dose J/Kg. The name of its SI unit is gray (Gy). The X-ray tube output was determined as a ratio of the incident air kerma to the tube current given by the equation.

$$\text{Tube output} = m(R)/\text{mAs} \quad (1)$$

Where m(R) is the kerma and mAs is the exposure time and tube current. The variation in the output could be attributed to the waveform, anode material, filtration, and tube age and anode surface damage. An additional parameter measured include the fluence defined as the number of photons (or particles) passing through a unit cross-sectional area and is typically expressed in units of cm².

$$\text{Fluence} = D(N)/D(A) \quad (2)$$

Where D (N) is the number of photons and D (A) is the cross-sectional area of a sphere. The workload is evaluated by the following equation:

$$\text{Workload} = I \times t \times n_p \times n_i \times d \quad (3)$$

where I is the current used measured in milliamperage, t is defined as the exposure time in seconds, n_p represents the average number of patient, n_i is the number of images per patient which is six and d is the number of days per week which is five. Workload uses the SI units' mA-min/week [2].

The R/F sensor was positioned in the path of the X-ray beam 115 cm from the X-ray source at varied orientation along the collimated area. With an uncertainty of 5% or 5 Gy, kVp 2% and time 0.5% with an overall error (inherent error) of 0.03%. The collimated area is set at various sizes for the different examinations barium meal (B.M) and intravenous pyelogram (IVP). The exposure is made, and the parameters are recorded from X 2 base unit. The tube output and fluence are calculated using the equation given above. The same process is repeated at 60 cm and 115 cm varied peak kilovoltage (50-125 kVp) and milliamperage (2-200 mAs). Kerma in air was to be assessed along with the incident kerma after interaction with the patient at the SID of 115 cm and 60 cm to show if the response values will be the half. Peak kilovoltage values at 90 kVp and 25 mAs were recorded after approximately one year.

Experimental

The aim of this work is to present a systematic and practical approach for the determination of calibration cycles. This study was carried out in two hospitals in Guyana namely Georgetown Public Hospital Corporation and Linden Hospital Complex with two different workloads and ages of X-ray tubes. The study was carried out with the assistance of a radiographer for each hospital [3].

The research was divided into the following phases. Incident air kerma was measured using Unfors RaySafe X2 with model number 1506035. The last calibration date of the RaySafe X2 is March 2017. The R/F sensor was positioned along the periphery and center of the collimated area at a distance 115 cm and 60 cm from the X-ray focal spot (Figures 1 and 2) [4].

Hospital and their respective analysis/examination

Georgetown Public Hospital Corporation (GPHC)

Barium Meal

Intravenous Pyelogram

Linden Hospital Complex (LHC)

Peak Kilovoltage

Tube Output

Source to R/F sensor

Materials

Siemens Fusion Luminous Fluoroscopy

Raymax Medical Corporation

Unfors RaySafe X2 Sensor Model number (1506035)

X2 view software

Auxiliary tools

Meter rule (3 m)

Spirit level



Figure 1: Unfors RaySafe X2 used in this study.

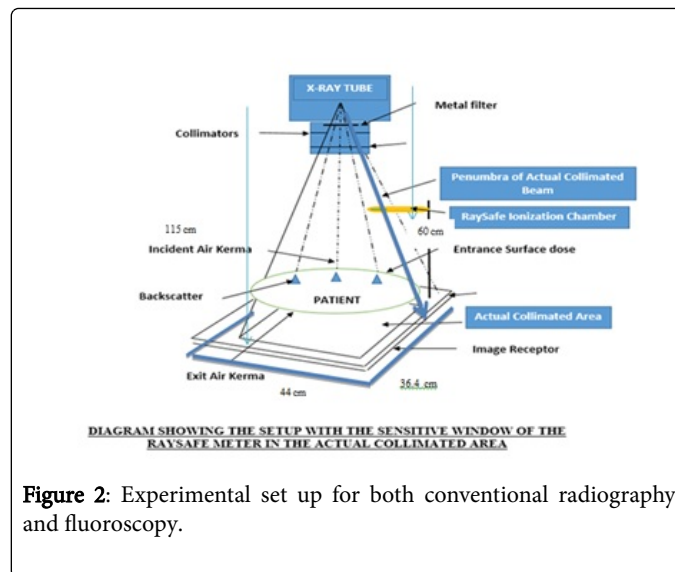


Figure 2: Experimental set up for both conventional radiography and fluoroscopy.

Results

The present study investigates kerma, X-ray tube output and fluence as shown in Figure 3 above. These factors were examined to establish comparative analysis of the X-ray tube's performance for each case, i.e. conventional versus fluoroscopic tube used for static exposures. Electro-technical factors of the first intravenous pyelograms (IVP), A was 80 kVp and 28 mAs, whilst parameters for the second examination were 70 kVp and 25 mAs.

This small difference in 3 mAs accounted for increasing attenuation due to patient's thickness, however resulted in increased photon production (Table 1). Peak kerma values for IVP A were 0.118 mGy and 0.068 mGy, while IVP B co-corresponded to 0.061 mGy and 0.053 mGy. A change of 10 kVp and 3 mAs would increase the number of photons produced and the penetrating power of the beam (Figures 3 and 4).

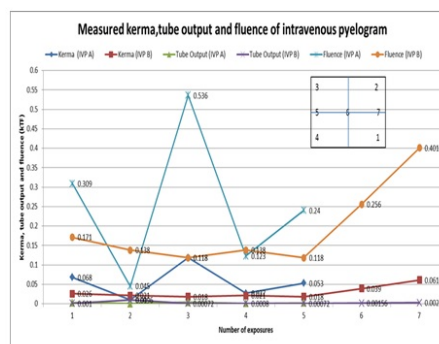


Figure 3: Comparison of kerma, tube output and fluence of an intravenous pyelogram.

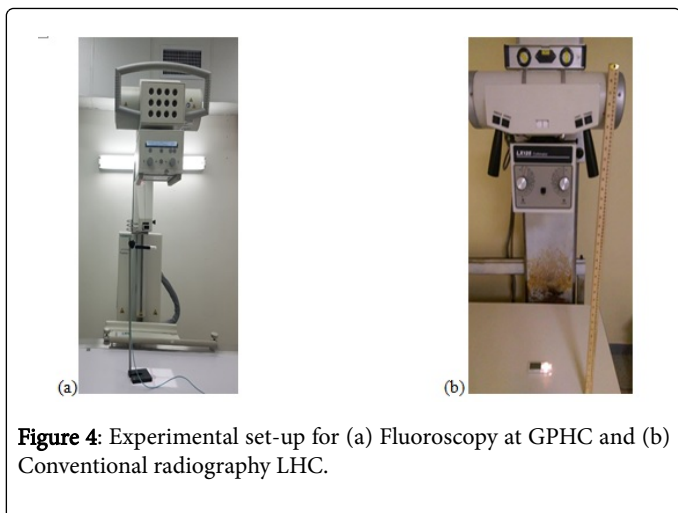


Figure 4: Experimental set-up for (a) Fluoroscopy at GPHC and (b) Conventional radiography LHC.

Facility	GPHC Siemens Luminos Fusion	Linden Hospital Complex Raymax Medical Corporation
Manufacturer model number	3345209	2136
Serial number	409161572	2878
Year manufacture of	April, 2015	May 04
Year installation of	February, 2016	2008
Anode angle	14.6	9.4
Workload	50	25
Age of tube	1 year	9 years
Tube heating	33700	33700

Table 1: Specific data of X-ray machines investigated.

Higher tube outputs were calculated for IVP A because of the higher kVp and mAs. At 80 kVp the outputs are 0.0024-0.0018 mGy/mAs. PA Oluwafisoye, CJ Olowookere showed tube output values ranging from 0.0318 mGy/mAs -0.119 mGy/mAs. The variation in output could be attributed to anode material, anode surface damage, filtration and waveform. The anode material used on the Siemens Luminos Fusion Fluoroscopy is tungsten which has high melting point of 3370°C and low rate of evaporation. Alloy containing tungsten and rhenium is also used, since 5-10% of rhenium prevents crazing of the anode surface [5-10].

The combination of inherent filtration plus added filtration equals total filtration. The determining factor for the total filtration is determined by the peak kilovoltage of an X-ray unit. The minimum total filtration for mobile diagnostic and/or fluoroscopic units is 2.5 mm Al (Deena Misner).

The following formula is proposed for the fluence:

$$\text{Fluence} = (D(N)) / (D(A))$$

Fluence was calculated at a distance of 1.15 m. IVP examinations were performed using distinct collimated areas of (44 cm × 36.4 cm) and (29.2 cm × 26.2 cm) respectively which is equivalent to exposed

areas of 1601.6 cm² and 765.04 cm² respectively. These areas represent the exposed area of incidence of all the X-ray photons with sufficient energy to traverse the patient. The first IVP examination used an exposed surface area of more than twice that of the second for photon distribution. Given that the surface of interaction of the homogenous photon beam is irregular shape, an equivalent sphere was used in keeping with equation 2 [11-15].

Volume of the prism for IVP A equaled 0.091 m³ compared to 0.044 m³ of IVP B. Radius of the sphere was 0.275 m compared to 0.215 m, while cross-sectional area of the sphere was 0.237 m² and 0.138 m². Fluence values varied from 0.539 mGy/m² to 0.045 mGy/m². Higher fluence values at positions 1,3 and 6 denote the cathode end which displayed the anode heel effect.

Lower values at positions 2 and 4 can only be as a result of increased scattered radiation and absorption by patient. The anode heel effect is a variation of the intensity of X-rays emitted by the anode depending on the direction of the emission. X-rays emitted towards the cathode are in general more intense than those emitted perpendicular to the cathode-anode axis.

Another parameter related to the fluence is the filtration which reduces the absorbed dose by filtering the low energy photons (hardening the beam), and increasing the average energy of the photons (Figure 5).

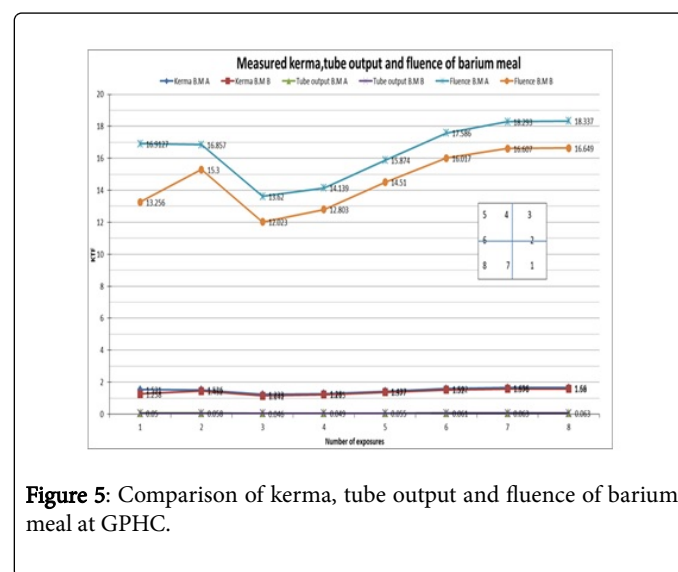


Figure 5: Comparison of kerma, tube output and fluence of barium meal at GPHC.

Kerma

Kerma measured at 115 cm by the R/F sensor in the path of the X-ray beam. Both examinations occurred at 25 mAs, 85 kVp and 83 kVp respectively. Collimated area was 27.2 cm × 26.2 cm and 29.2 cm × 26.2 cm for examination A and B respectively. Positions six, seven, and eight, displayed higher values for both examinations, but barium meal A had a higher intensity. Peak kerma values were 1.66 mGy and 1.58 mGy for BM A and BM B. Lowest value was obtained at position 1 indicative of the position of the anode heel effect. Average kerma values of BM A and BM B are 1.489 mGy and 1.389 mGy respectively with an increase of 0.10 mGy [16-20].

Tube output

BM A recorded a peak X-ray tube output of 0.066 compared to 0.063 of BM B. Peak values occurred at positions six, seven and eight. This is due to less patient attenuation and less scatter. Average tube output was 0.059 mGy/mAs and 0.055 mGy/mAs. The variation in output could be attributed to anode material, anode surface damage, filtration, and waveform. The anode material is tungsten however due to the unit being one year old the surface damage is minimal. The electro-technical factors used did not produce any significant deviation or outlier with the set milliamperage being 25 for both examinations.

Fluence

The fluence was calculated at a distance of 115 cm. Collimated area of barium A was 27 cm × 26.2 cm versus 29.2 cm × 26.2 cm of examination B. Comparing the results of examinations A and B showed the volume of prism to be 20488.4 cm³ and 21995.5 cm³, while radius of sphere equaled 16.97 cm and 17.3 cm respectively. Cross-sectional areas of the sphere were 905.237 cm² and 948.96 cm² for barium meal A and B respectively. The fluence varied from 0.565 mGy/cm² to 18.337 mGy/cm². Barium meal A had a higher fluence value of 18.337 compared to 16.649 because of the smaller collimated area. Greater fluence values were calculated at positions seven, eight and nine for both examinations which were indicative of the anode heel effect and less scattered radiation (Figure 6a) [21-25].

Experiments done without patients were divided into four sections; measurements at 115 cm and 60 cm, varied kVp, mAs and kVp measurements after 24 weeks from February 2016 to August 2016 and 64 weeks from February 2016 to August 2017. Therefore no absorbed dose and 100% of the measured values occurred in air (Figure 6b).

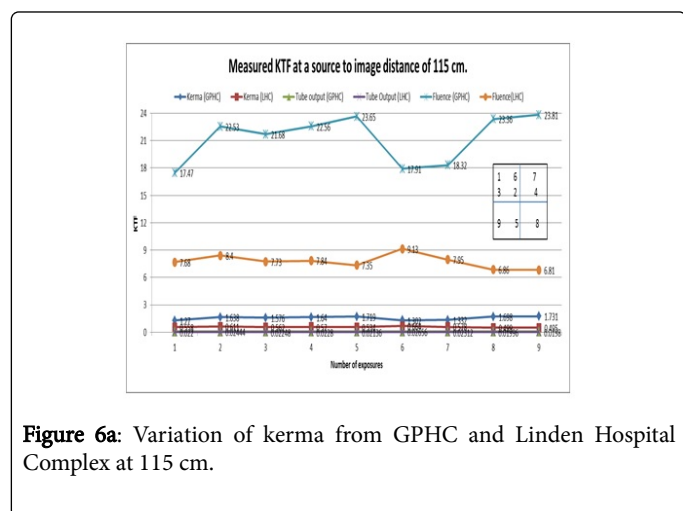


Figure 6a: Variation of kerma from GPHC and Linden Hospital Complex at 115 cm.

Kerma

Comparing two X-ray tubes at different workloads and tube age at 115 cm. Figure 6a measured kerma at 115 cm away from source using R/F sensor. Parameters set included 90 kVp and 25 mAs. At 115 cm the maximum kerma measured was 1.731 compared to 0.664 at Linden Hospital Complex. A collimated area of 27 cm x 17 cm was used. Position five, eight and nine displayed peak values for GPHC, at the same time positions two and six showed peak values for LHC. GPHC on average was 2.7 times greater compared to LHC. Factors responsible for this include the age of the X-ray tube, anode pitting and anode heel

effect, angle of the anode and filtration. Positions five, eight and nine displayed the anode heel effect with more photons deposit at the cathode end [26].

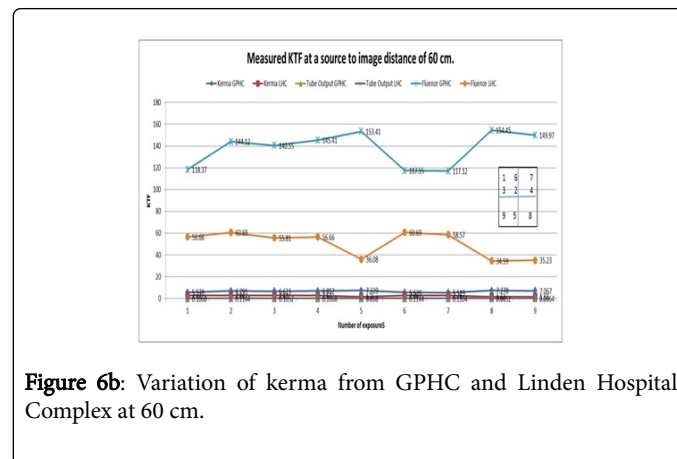


Figure 6b: Variation of kerma from GPHC and Linden Hospital Complex at 60 cm.

GPHC was commissioned in February, 2016 compared to 2008 of LHC resulting in less deterioration of target track. GPHC exhibited an anode angle of 14.60 compared to 9.40 at LHC this smaller angle limits the useable X-ray field. The amount of filtration of the X-ray beam is based on the voltage potential (keV) used to produce the beam. Governmental regulations require the total filtration to be 2.5 mm aluminum for all higher voltage (above 70 kVp) (Serman).

The higher the kVp the less radiation is absorbed by the patient. The aluminum as a choice removes many of the lower energy (long waves) photons with lesser effect on the higher energy photons which penetrate to the film. GPHC X-ray unit was equipped with 2.5 mm Al versus 1.5 mm at LHC.

Tube output

Peak tube output occurred at positions five, eight, nine and two and six for GPHC and LHC respectively on Figure 6a. Average tube output for GPHC was 0.06 mGy/mAs compared 0.02 mGy/mAs for LHC, three times greater than of the increase production of photons this implies the efficiency of the production of photons and the increase in anode angle 4.6 allowing a more divergent beam with more points of interaction and photons. Factors influencing the tube output include tube voltage and waveform. GPHC acquired higher tube output because of the higher radiation produced compared to LHC.

Tube output

Maximum kerma values were 0.289, 0.291 and 0.283 mGy/mAs for GPHC and 0.114 for LHC which was indicative of Figure 6b. Average tube output is 0.259 and 0.095 mGy/mAs for the two X-ray units. Factors affecting the tube output include waveform. At the elevated level 60 cm away from the source the X-ray tube output are greater when compared to 115 cm because of the photons having a less distance to travel. The age of the X-ray and the workload with the GPHC tube being newer, but having a higher workload still resulted in the tube output being higher.

Fluence

Figure 6a shows fluence was calculated at a distance of 115 cm. A collimated area of 27 cm × 19 cm was used. The peak fluence occurred

at positions five, eight and nine contrasting positions two and six of LHC. Average fluence equaled 21.25 mGy/cm² and 7.75 mGy/cm² for GPHC and LHC respectively. The age of the X-ray tube being 1 year at GPHC compared to 9 years at LHC resulted in the fluence being approximately 1/3 denoting one third lost in the amount of electrons in the anode over a 9 year period.

Anode angle calculated were 14.60 and 9.40. Smaller the angle the smaller the focal spot which limits the size of the useable X-ray field owing to cutoff. There were no patients, thus no scatter and attenuation. The Siemens possesses an automatic sensor for higher energy level above 75 kVp to from 2.5 mm Al to 3.1 mm Al for the RayMax unit there is no automatic sensor [27,28].

Figure 6b shows fluence at the elevated level of 60 cm. Average fluence equaled 137.88 mGy/mAs and 50.55 mGy/mAs. Because of the elevated level of the R/F sensor values were 6.4 times greater when compared at the 115 cm. At the elevated the cross-sectional area of the sphere 471.78 cm² when compared to 726.78 cm² at 115 cm. Anode angle calculated were 14.60 and 9.40. Smaller the angle the smaller the focal spot which limits the size of the useable X-ray field owing to cutoff. There were no patients, thus no scatter and attenuation. In addition less anode surface damage for the newer tube.

The X-ray unit possessed two different filtering size 2.5 mm Al and 1.5 mm Al based on the operating kVp of the unit. Increased peak kilovoltage causes the filter of Siemens unit to automatically increase from 2.5 mm to 3.1 mm Al. In conclusion the Siemens unit produced more photons per cm² based on the number of photons produced in the cathode and the age influencing the target track deterioration also as crazing which causes network of fine cracks along the anode surface (Figure 7).

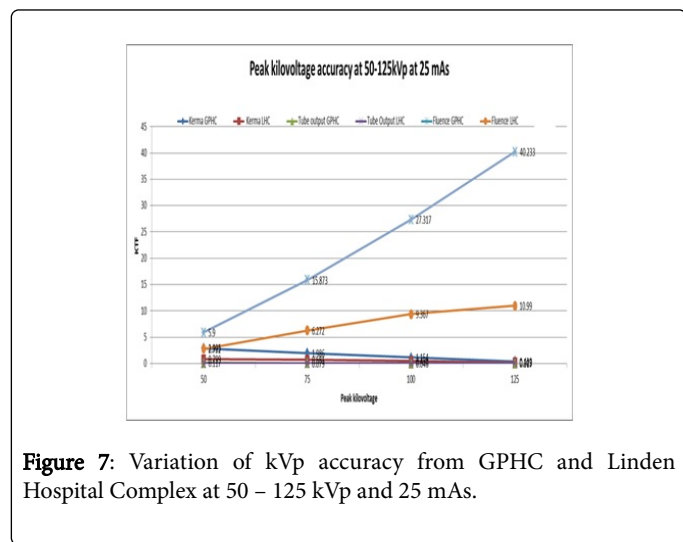


Figure 7: Variation of kVp accuracy from GPHC and Linden Hospital Complex at 50 – 125 kVp and 25 mAs.

Kerma

Kerma 2.925, 1.986, 1.154, 0.429 mGy for GPHC and 0.799, 0.681, 0.456, 0.203 for LHC. An increase in kVp caused an increase in kerma. Average kerma for GPHC was 1.623 mGy compared to 0.534 at LHC. Comparing two X-ray tubes of different workloads. The kerma was measured using the RaySafe R/F sensor. The tube potential was set between 50 kVp- 125 kVp and increased in steps of 25 kVp at 25 mAs. The greater the potential difference the faster the electrons travel from the cathode to the anode. This result in an increased efficiency of

conversion of electron energy into X-ray photons and thus an increase in the number of photon kerma generated. As the kVp is increased, mAs held constant there is a corresponding increase in the mean energy of the beam, total number of photons emitted and the maximal energy of the photons [29,30].

Tube output

Average tube output was 0.06475 mGy/mAs at GPHC compared to 0.02139 mGy/mAs at LHC with varying kVp. The tube output is affected by the waveform, anode angle, collimation, tube current. Anode angles of 14.6 and 9.4 corresponded to GPHC and LHC respectively. The anode angle controls the degree of X-ray absorption in the anode material. LHC has an angle of 9.4 owing to increase in the absorption length within the target when compared to GPHC. The smaller angles limit the size of the useable X-ray field owing to cutoff. The collimated area was 27 cm × 19 cm for both X-ray tubes (Figure 8).

Fluence

Average tube output was 22.33075 mGy/cm² at GPHC compared to 7.35525 mGy/cm². For fluence, the volume of the triangular prism equaled 14748.7 cm³. Radius of the sphere was 15.21 cm and cross-sectional area of the sphere being 726.78 cm. Higher kVp corresponded to higher fluence because of the increase in intensity of the X-ray photons. Higher kVp also accounted for more scattered radiation [31].

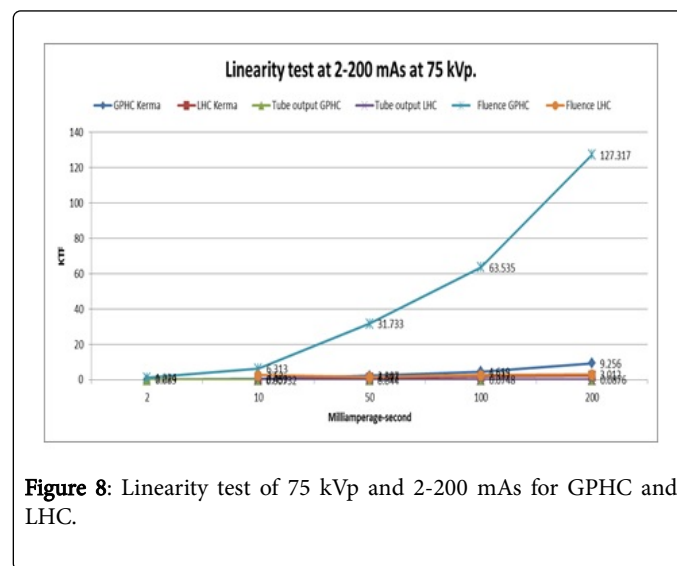


Figure 8: Linearity test of 75 kVp and 2-200 mAs for GPHC and LHC.

Kerma

Kerma measured at 115 cm away from the source. Parameters set for this analysis was 75 kVp and varying mAs of 2-200. Collimated area was defined as 27 cm × 19 cm. The mAs determine the number of photon produced. Higher mAs produced more X-ray photon (radiation), conversely lower mAs produces less photons. Peak kerma values were measured at 200 mAs for both facilities. Peak kerma was 9.256 mGy compared to 2.19 mGy this can attributed to the age of the X-ray tube and less deterioration of the target track. At two mAs GPHC registered a value of 0.089 mGy versus no data at Linden Hospital Complex. Average kerma was 3.346 mGy and 1.33 mGy of GPHC and LHC respectively.

Kerma depicted on Figure 6b at an elevated level of 60 cm values were 7.278 mGy against 2.86 mGy achieved at LHC. The average kerma values of GPHC were 6.497 mGy and 2.38 mGy at LHC. The elevated height of the R/F sensor curtailed the distance of the X-ray source to the sensor therefore generating a higher kerma value. GPHC values were 2.7 times greater than those acquired at LHC. Greater kerma values were measured at positions five, eight and nine for GPHC, with positions two and six for LHC. The elevated height of 60 cm had a greater kerma because of the reduced distance the photons had to travel to reach the R/F sensor.

Tube output

The tube output is affected by the milliamperage/second, wave form and tube voltage. In this analysis the tube voltage was held constant at 75 kVp only varying parameter was the mAs. An increase in the mAs cause an increase in the number of photons, therefore decreasing the tube output. As seen by the graph the GPHC produce a lower tube output because of the increase in radiation. Calculated tube output at 200 mAs was 0.0876 mGy/mAs and 0.0462 mGy/mAs for LHC and GPHC respectively (Tables 2 and 3) [32].

Fluence

Greater mAs corresponded to higher fluence because of the increase in number of photons per cm². For fluence, the volume of the triangular prism ref to Figure 5 with project field: equaled 14748.7 cm³. Radius of the sphere was 15.21 cm and cross-sectional area of the sphere being 726.78 cm². Although the anode angle was greater at GPHC fluence values were higher which allowed for more radiation of the useable beam. At two mAs GPHC registered a fluence of 1.224 mGy/cm² × 10⁻⁴ while LHC did not register a value. Peak fluence was 127.317 mGy/cm² × 10⁻⁴ and 3.0 mGy/cm² × 10⁻⁴ therefore the higher the mAs the greater the number of photons produced and higher the fluence (Figure 9).

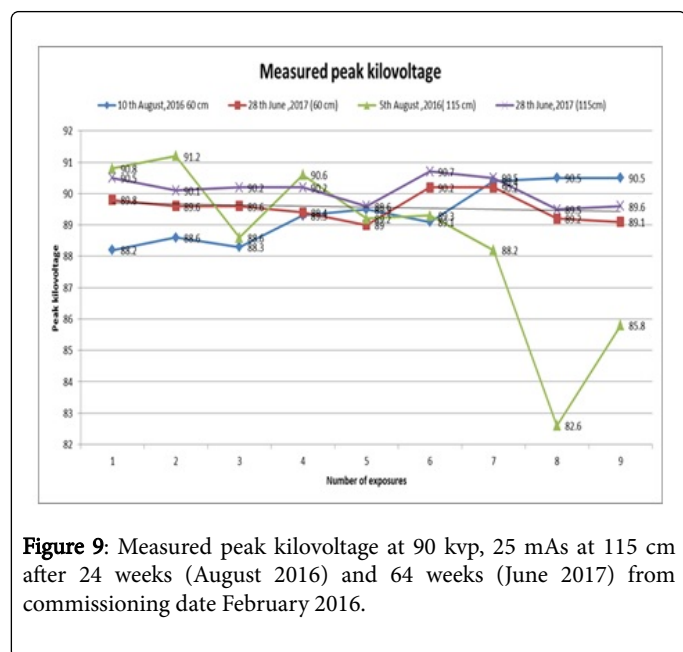


Figure 9: Measured peak kilovoltage at 90 kVp, 25 mAs at 115 cm after 24 weeks (August 2016) and 64 weeks (June 2017) from commissioning date February 2016.

Peak kilovoltage

Measured data at 115 cm for August 2016 and June 2017. The electro-technical factors set for this examination were 90 kVp and 25 mAs. Descriptive statistics showed a mean of 88.4 kVp and 34.2 ms, and standard deviation of 2.74 for August 2016, which was 24 weeks after commissioning. The average delay between measurements accounted for 228 minutes. The highest kVp was measured to be 91.2 and taken at a time delay of 4 min. Results for June 2017, 64 weeks after commissioning mean kVp exposure time and standard deviation are 90.1, 33.3 ms and 0.4 respectively. The average time delay between measurements 78 minutes.

Statistical Parameters	5 th August, 2016 (24 weeks)	28 th June, 2017 (64 weeks)
Average kVp	88.4	90.1
Time (milli-seconds)	34.2	33.1
Standard deviation	2.74	0.4
Time between measurements	228	78

Table 2: Statistical parameters taken into account after 9 exposures at 115 cm.

Statistical Analytical Parameter	5 th August, 2016	28 th June, 2017
Average kVp	89.3	89.5
Time (milli-seconds)	34.1	33.3
Standard deviation	0.9	0.4
Time between measurements	42	150

Table 3: Statistical parameters taken into account after 9 exposures at 60 cm.

The highest kVp was 90.7. Changes in the x ray spectrum are a result of increased exposure time while tube current (mA) and tube voltage (kVp) remain constant. The amount of radiation the patient received is determined by the mAs. The kVp was kept constant in this procedure. The kVp determines the number of photons generated, mean energy and maximal energy. An increase of 1.7 kVp occurred from August, 2016 to June 2017. Kilovoltage peaks were found to be closer to mean for June, 2017 results which highlighted the consistency of X-ray tube after 2400 exposures.

After one year of use the X-ray tube worked more efficiently and was adapted to the workload. Better production of photons via particles remaining in an energetic state faster than when the tube was new, therefore demanding less time delay and less energy to produce X-ray photons of the same energy range. Measurements at 60 cm since August, 2016 compared to June 2017. Mean of kVp, exposure length and standard deviation for August, 2016 are 89.3, 34.1 ms, and 0.9 respectively at an elevated level 60 cm 24 weeks after commissioning. Average time delay between measurements was 0.7 minutes.

Results for June, 2017, showed a mean kVp, exposures time, and standard deviation of 89.5, 33.3 ms and 0.4. Time delay between measurements is 150 second with 13 minutes being the delay for exposure one which accounted for a kVp of 90.5. There was an increase of 0.2 kVp, 16 months after commissioning and 3,840 exposures. At the

elevated height of 60 cm after 64 weeks the X-ray tube was found to be functioning more efficiently because the less energy is required for ionization.

Workload

Radiation is not produce 24 hours per day, 7 days per week the parameter which best describe this relationship of the weekly radiation use of the X-ray tube is called the workload.

$$\text{Workload} = I \times t \times n \times p \times n_i \times d \quad (3)$$

Units for workload are either milliamperage-seconds (mAs)/week or milliamperage-min (mA-min)/week. The workload varies greatly with assumed maximum kVp and is usually a gross overestimation. The average workload for a radiographic room is 277 mA-min/week. The estimated workload based on this study is 25 mA-min/week based on a 5 day work week and 25 milliamperes.

Number of exposures

Under special examinations barium meal and intravenous pyelograms the total number of patients per month was found to be 41 specifically 30 barium meals and 11 intravenous pyelograms. The number of days used was five compared to standard seven days. Numbers of exposures were averaged to be six per patient based on the intravenous pyelogram and barium meal procedures. Commissioning was done February, 2016 and was compared to data from August 2016 and June 2017. Number of exposures after commissioning 1,440 exposures (24 weeks) compared to 3,840 after 64 weeks (June 2017).

Conclusion

This research investigated the effect of variation factor on the calibration of the static radiography on a fluoroscopy unit. Factors measured were kerma, tube output, fluence and age of tube output and workload. The differences obtained were significant in the cases of Linden Hospital Complex vs Georgetown Public Hospital and 115 cm versus 60 cm. The difference in tube output could be attributed the anode surface damage, age of the tube, filtration and collimated area.

It can be concluded that facilities with workload of approximately 50 patients do not require more frequent calibration consequently lower workload require less calibration. The optimal time for calibration then can be defined as 18 months for hospitals with over 50 patients and 24 months for facilities with less than 50 patients.

Acknowledgements

The author wishes to thank Georgetown Public Hospital Corporation and Linden Hospital Complex for their participation in this analysis, faculty advisor Ms. Petal Surujpaul MSc. Medical Physics BSc. Physics for her guidance, and the radiographers who collaborated in the procurement of data on technical factors.

References

1. Peixoto JGP, Almeida CE (2002) Implementation of a mammography calibration system. *Radiat Prot Dosimetry* 1: 33.
2. Matthews K, Brennan PC (2009) The application of diagnostic reference levels: General principles and an Irish perspective. *Radiography* 15: 171-178.
3. Vassileva J (2015) Diagnostic reference level. *Am. J. Roentgenol* 204: W1-W3.
4. (2001) Diagnostic reference levels in medical imaging: Review and additional advice. *Ann ICRP* 31: 33-52.
5. Serman N (2018) Production of X-rays and interactions of X-rays with matter 11-20.
6. (2002) Particular requirements for the safety of X-ray equipment for computed tomography. Geneva.
7. (2008) The measurement, reporting and management of radiation dose in CT, Maryland.
8. (1999) Radiation protection 109: Guidance on diagnostic reference levels for medical exposures (radiation protection). Directorate-General, Environment, Nuclear Safety and Civil Protection, Europe.
9. Bushberg JT, Seibert JA, Leidholdt EM, Boone JM (2002) The essential physics of medical imaging: Lippincott Williams & Wilkins, Philadelphia.
10. (2013) International Atomic Energy Agency.
11. Cynthia MCH (2018) Diagnostic reference levels. *Image Wisely. Radiation safety in adult medical imaging.*
12. Cynthia MCH (2010) Diagnostic reference levels. *Image Wisely. Radiation safety in adult medical imaging.*
13. Simpkin DJ (1991) Shielding a spectrum of workloads in diagnostic radiology. *Health Phys* 61: 259-269.
14. (2007) Dosimetry in diagnostic radiology: An international code of practice. Vienna.
15. Douglas SJ (2008) Overview and basis of design for NCRP report 147. Milwaukee.
16. Esien EM (2012) Determination of workload and use factor in the general radiography room of a major nigerian teaching hospital. *Nig J Med Imag Rad Ther.*
17. (2011) Patient dose: What to record and track and the role of organ dose 6-13.
18. Harold E, John CJR (1983) *Physics of Radiography* Richmond: Charles C Thomas Publishers Ltd, USA.
19. (2007) Implementation of the international code of practice on dosimetry in diagnostic radiology (TRS 457). Review of test results. *IAEA Human Health Reports* 129.
20. Kadhim RM (2011) Estimation of Entrance Surface Air Kerma (ESAK) and dose area product (DAP) for the patient examined by fluoroscopy apparatus [long term X-ray examination]. *Kerbala University* 9.
21. Leitz W, Axelsson B, Szendro G (1995) Computed tomography dose assessment: A practical approach. *Radiation Protection Dosimetry* 57: 337-380.
22. (2011) Specialist in radiation protection. *Health Physics Society.*
23. Oliveira LC, Dias TK, Lopes RT, Kodlulovich S (2009) Evaluation of the entrance surface air kerma in mammographic examinations in Rio de Janeiro, Brazil. *Radiat Prot Dosimetry* 133: 136-143.
24. Oluwafisoye PA, Olowookere CJ, Tobaskeho NNJ (2010) Quality control and environmental assessment of equipment used in diagnostic radiology. *IJRRAS* 148-158.
25. Patel V, Highnam R, Tromans C, Pizzutiello RJ, Destounis S (2013) Patient specific average glandular dose in mammography. *Int J Med Phy Res Prac* 40.
26. (2012) Radiation protection in medicine: Setting the scene for the next decade. International Atomic Energy Agency (IAEA).
27. (2014) Radiation protection and safety of radiation sources: International Basic Safety Standards. Vienna 436.
28. Harding K, Thomson WH (1997) Radiological protection and safety in medicine: ICRP publication 73. *Eur J Nucl Med* 24: 1207-1209.
29. Statkiewicz MSA (2011) Radiation protection in medical radiography Maryland heights, Mosby.
30. Suliman II, Elshiekh EHA (2008) Radiation doses from some common pediatric X-ray examination in Sudan. *Radiat Prot Dosimetry* 64-72.

31. Taha TM (2010) Study the quality assurance of conventional X-ray machines using non-invasive KV meter. Radiation Protection Department, Nuclear Research Center. Cairo 105-110.
32. Zoetelief J, van Soldt RTM, Suliman II, Jansen JTM, Bosmans H (2006) Quality control of equipment used in digital and interventional radiology *Radiat Prot Dosimetry* 117: 277-282.